ELSEVIER

Coastal Engineering 37 (1999) 259–282

COASTAL ENGINEERING

www.elsevier.com/locate/coastaleng

# Evaluation of high frequency radar wave measurement

L.R. Wyatt *, S.P. Thompson, R.R. Burton

*Sheffield Centre for Earth Observation Science, School of Mathematics and Statistics, Sheffield University, Hounsfield Road, Hicks Building, Sheffield S3 7RH, UK*

**Abstract**

The spatial coverage, temporal availability and spectral and parameter accuracy of wave measurements using radars operating at the upper end of the high frequency (HF) radio band are discussed. The two radars used are the Ocean Surface Current Radar (OSCR) developed in the UK and the Wellen Radar (WERA) developed in Germany. The measurements show that useful accuracy is obtainable with very good potential for operational coastal monitoring. Direction biases over most of the frequency range are less than 15°. The relative bias in significant waveheight estimation in high sea-states is within ±5%. Although there is some deterioration in spectral performance in high sea-states, this is primarily confined to amplitudes at the higher ocean wave frequencies where a modelling approach could be adopted. Gaps in spatial and temporal coverage and some reduction in accuracy in mean direction estimation are due to surface current variability or antenna sidelobes. 

*Keywords:* HF radar; OSCR; WERA; Wave measurement; Directional spectrum

## 1. Introduction

High frequency (HF) radar systems have the capacity for measuring both directional wave spectra (Wyatt, 1990a; Wyatt and Holden, 1992; Wyatt and Ledgard, 1996) and surface currents over a wide area of the coastal ocean, providing for the first time a means of monitoring the simultaneous spatial and temporal variability of waves and currents (Paduan and Graber, 1997). This paper concentrates on the wave measurement capability. Current measurement is discussed elsewhere (Gurgel et al., 1999). The processing of the signal received by the radar provides a measure of the backscattered

* Corresponding author. Fax: +44-114-22-23739; E-mail: l.wyatt@sheffield.ac.uk

0378-3839/99/$ - see front matter 
PII: S0378-3839(99)00029-0

power from a number of cells roughly 1 $km^2$ in area (up to 700 with the Ocean Surface Current Radar [OSCR] system, Wyatt and Ledgard, 1996) on the ocean surface. Wave and current measurements are obtained from the power spectrum of the backscattered signal.

Fig. 1 shows an example of wave variability, in space, time and frequency, measured using OSCR at Holderness (Prandle et al., 1996). The figure shows differences in mean wave direction and energy levels in three different frequency bands associated with the change in wind direction shown in the upper row. It also shows spatial variability in these parameters within each frequency band. An hour or so before the beginning of the period shown here, winds were north-easterly and the front associated with the change to the south-easterly pattern seen at the later times here, is moving through the region from the west at 0100 h on 21/12/95. Note that although the high frequencies (in the second and third rows) show a great deal of variability as the front goes through, the longer waves (bottom row) are largely unaffected. The change to south-easterly winds is matched by the higher frequency waves with very little time delay (see the second row in the figure). By the end of the period, the effect of the wind has propagated to lower frequencies (3rd row) but not to the lowest frequency band shown here (bottom row) which contains predominantly swell waves being refracted towards the coast, although to the south there is some indication that the wind is beginning to influence the spectrum at these frequencies. Note that in these and all other figures in this paper, the convention used is that the direction is that towards which the waves (and wind) are propagating.

These are the sort of data that will be of great value for testing and developing numerical models of waves in shallow coastal waters. Operational monitoring of waves and currents is also feasible for a variety of coastal management applications, e.g., vehicle traffic services for commercial and leisure ports and harbours.

The wave measurements are made by inverting an integral equation that describes, with certain limitations, the relationship between the ocean wave directional spectrum and the power spectrum of the backscattered signal (Holden and Wyatt, 1992). The main limitation is a small slope assumption which essentially requires the waveheight to be small as compared to the radio wavelength. This approximation becomes increasingly invalid as the waveheight and/or radio frequency increases. Most HF radar systems that have been developed for current measurement operate at the upper end of the HF band where the assumptions made become questionable at waveheights above 2–3 m. A numerical technique developed by Wyatt (1990b) is used to carry out the inversion and this is also subject to some approximations. The equation is non-linear in the ocean wave directional spectrum and a linearisation is used to simplify the problem. This limits the inversion to frequencies less than about 0.36 Hz, beyond which a simple wave model (e.g., a $f^5$ decay) is used. The linearisation is a good approximation in higher sea-states but is less so in swell-dominated conditions. In fact, inversions of the full non-linear equation have been developed (Hisaki, 1996; Wyatt, 1996) but these do not appear to increase the accuracy of the solution.

The inversion produces directional wave spectra on a non-uniform grid of wavenumbers. These are averaged into wavenumber-direction bins, converted to directional frequency spectra using the dispersion relationship and then integrated to provide the frequency spectrum and parameters of the directional distribution, e.g., mean direction

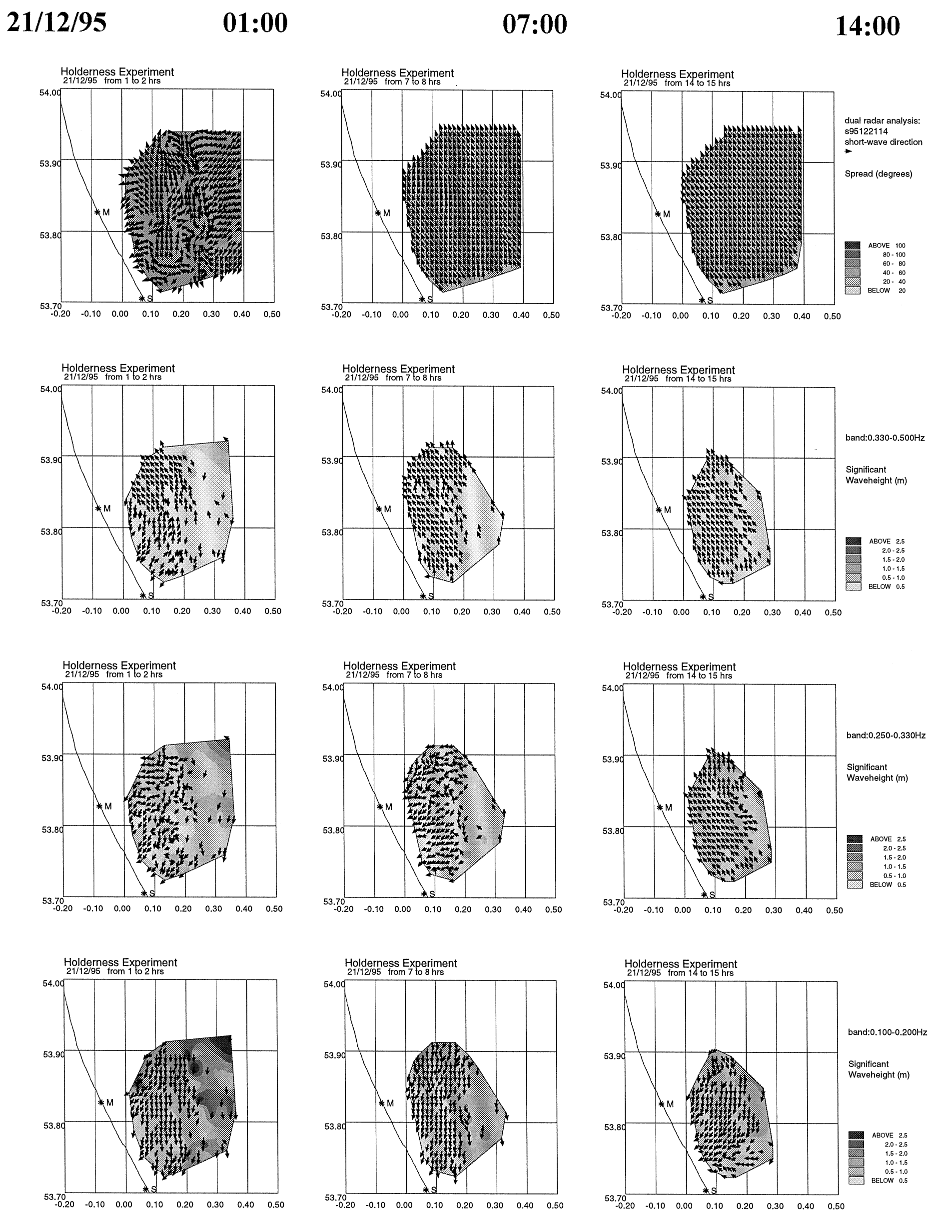


Fig. 1. Wave parameters measured at Holderness at three times on 21/12/95. The locations of the two radars that make up the OSCR system are shown as M and S. The upper panel shows wind (from short wave) direction with the arrows pointing in the direction that the wind is blowing. The directional spreading of short waves is also shown in grey shading. Note that the region of coverage for these parameters is larger than the rest. The other panels show mean direction (arrows towards which the waves are propagating) and amplitude in the frequency bands 0.33–0.5 Hz, 0.35–0.33 Hz and 0.1–0.2 Hz from top to bottom, respectively.

(a) Wind direction at Holderness

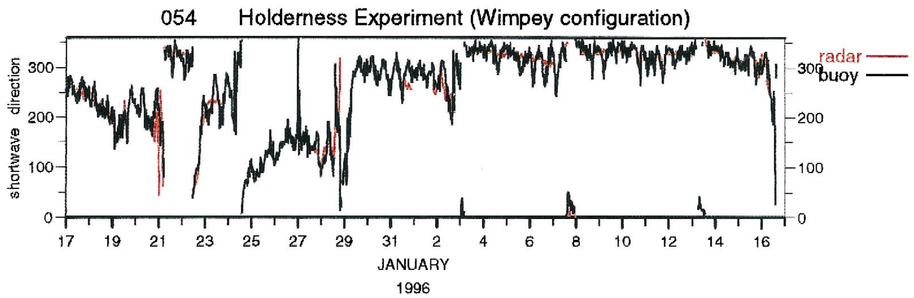


(b) Wind direction at Petten

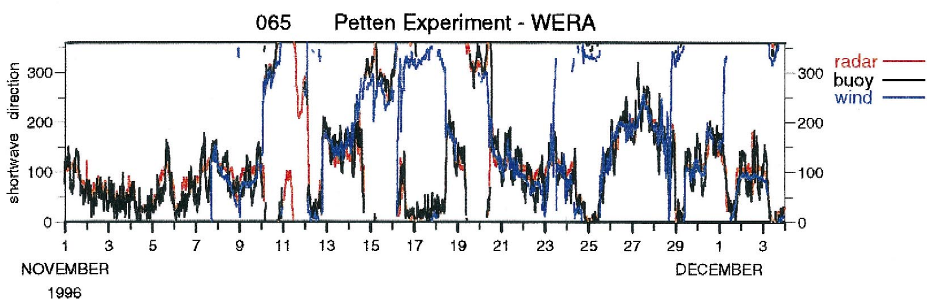


Fig. 2. Time series for Holderness (upper) and Petten (lower) of short wave and wind directions measured by the radar (red), a directional waverider (black) and, for Petten only, an onshore anemometer (blue).

as a function of frequency. Methods to analyse the spectra directly from the non-uniform grid have been developed (Isaac and Wyatt, 1997) but are not yet capable of handling large quantities of data in an operational way and hence, have not been used in this project.

Wind direction measurements are determined using a maximum likelihood (ML) model fitting approach (Wyatt et al., 1997). The two largest contributions to the backscattered spectrum are associated with waves of half the radio wavelength moving towards and away from the radar site. At the radar frequencies used in the work reported here, these waves have a frequency of about 0.5 Hz and hence, can be assumed to be aligned with the wind direction except in very low sea-states. The model determines the relative amplitude of the towards and away peaks in the spectrum and depends on two parameters, mean direction and directional spreading, the values of which are obtained using the ML method.

---

Fig. 3. Time series for Holderness (upper) and Petten (lower) of amplitude in three frequency bands: 0.05–0.4 Hz (and hence, significant waveheight), 0.2–0.4 Hz and peak. Radar measurements are in red and directional wavebuoy in black.

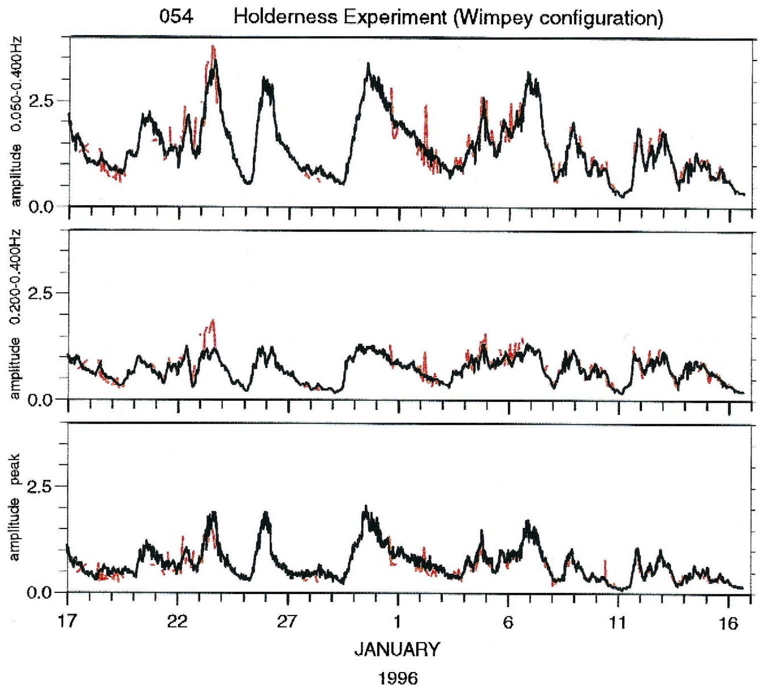
054 Holderness Experiment (Wimpey configuration)
amplitude 0.050-0.400Hz
amplitude 0.200-0.400Hz
amplitude peak
0.0
2.5
17
22
27
1
6
11
16
JANUARY
1996

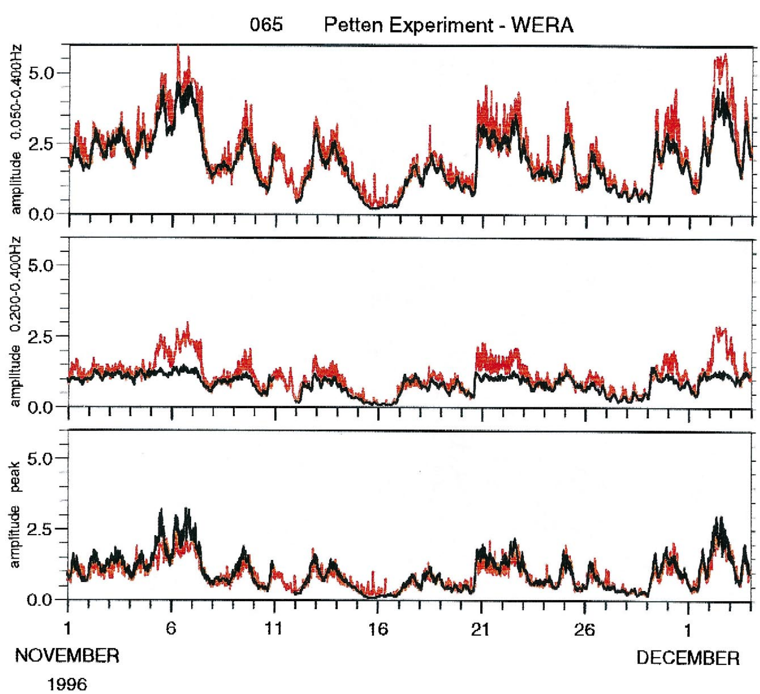
065 Petten Experiment - WERA
amplitude 0.050-0.400Hz
amplitude 0.200-0.400Hz
amplitude peak
0.0
2.5
5.0
1
6
11
16
21
26
1
NOVEMBER
1996
DECEMBER

In this paper, we discuss the accuracy and limitations of HF radar wave measurement for systems operating at the upper end of the HF band. The two systems are the OSCR, developed in the UK in the mid-eighties and until recently, available commercially for current measurement, and the Wellen Radar (WERA) developed by the University of Hamburg (Gurgel and Antonischki, 1997) as part of the SCAWVEX project. The data discussed in this paper were collected during two of the SCAWVEX experiments at Holderness, UK, and at Petten in the Netherlands.

## 2. The datasets

Krogstad et al. (1999) discuss various approaches to the problem of comparing data from instruments with different methods for measuring the same physical quantity (in this case, the wave spectrum) and different sampling variabilities. The methods are presented there and applied to the standard wave parameters significant waveheight, mean period and mean (spectrally averaged) direction. In this paper, the data are examined in more detail using a ML method (Sova, 1995) and relative or mean differences depending on the particular parameter under consideration. This approach provides quantitative information about the performance of the measurement technique. Before doing this, an overview of the datasets will be presented and important features of the comparisons highlighted.

Fig. 2 shows time series of radar-measured wind directions, using the Wyatt et al. (1997) method, during both experiments. At Holderness, they are compared to wave directions at the same frequency measured by a co-located Directional Waverider buoy. These are also shown for the Petten experiment where wind directions measured at the coast ( ~ 10 km away from the radar and buoy measurements) are also included. Note that the buoy measurements have not been compensated for surface current effects and these are thought to be contributing to the apparent tidal modulation of the buoy short wave direction measurements. Apart from this, agreement is generally very good even during periods of rapid change.

Fig. 3 shows time series of radar and wavebuoy amplitude (see Section 4.1 for the definition of amplitude used here) for the Holderness and Petten experiments. Mean direction and mean period are shown in Figs. 4 and 5, respectively. The amplitude, direction and period estimates at high frequencies and at the peak of the spectrum are also shown. Note that the sampling variability (not shown) associated with estimates of the peak parameters is large and so more scatter between the two measurements is expected. The qualitative agreement between radar and wavebuoy is good in general. The most obvious difference between the two experiments is the continuity in radar measurements at Petten and the relative sparseness at Holderness. This is related to the data collection capabilities of the systems used which, for OSCR, were limited by old computer hardware. The Petten experiment demonstrated that HF radar is capable of measuring wave statistics on a regular basis. WERA backscatter measurements were made every 20 min but there were occasional gaps in wave measurement at particular locations when the quality of the radar measurements was not sufficient. These cannot be identified in these time series plots because the gaps in time between good quality

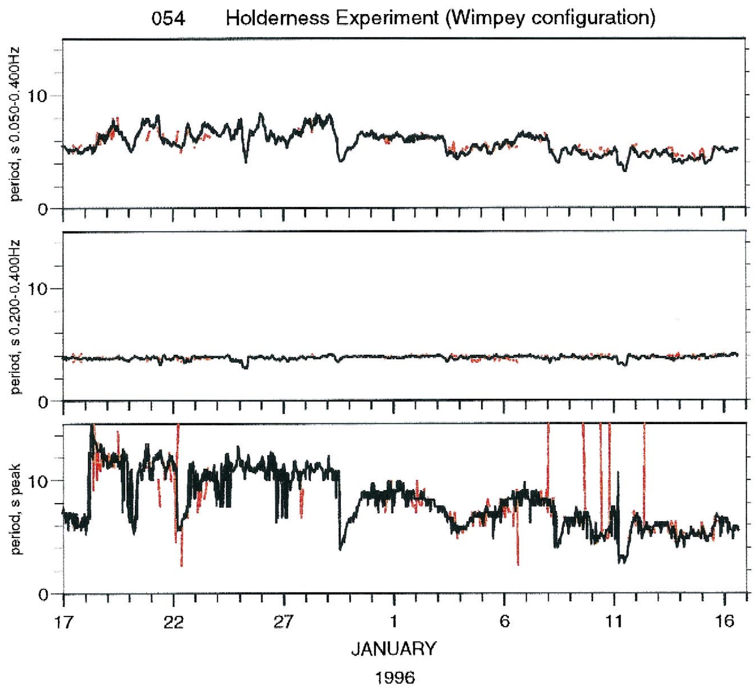


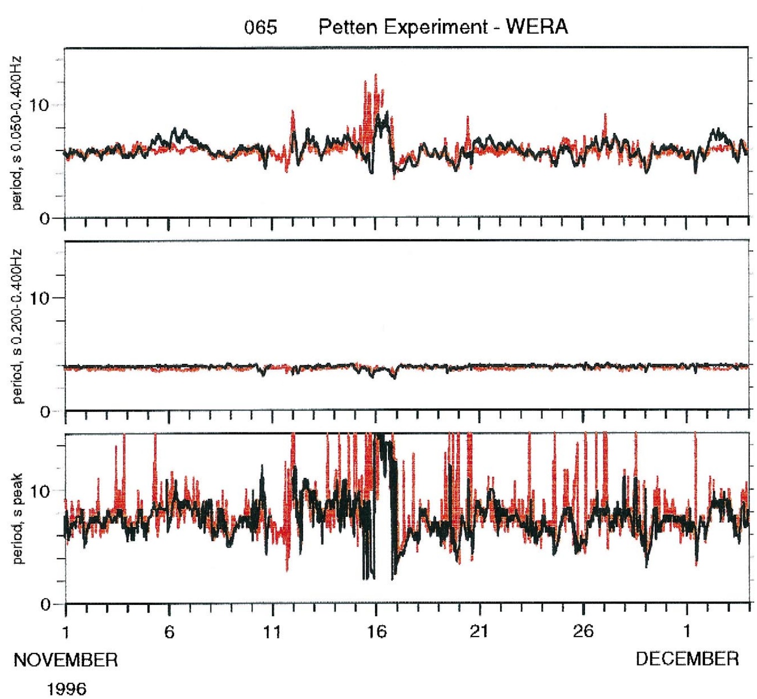


Fig. 4. As Fig. 3 for mean period.

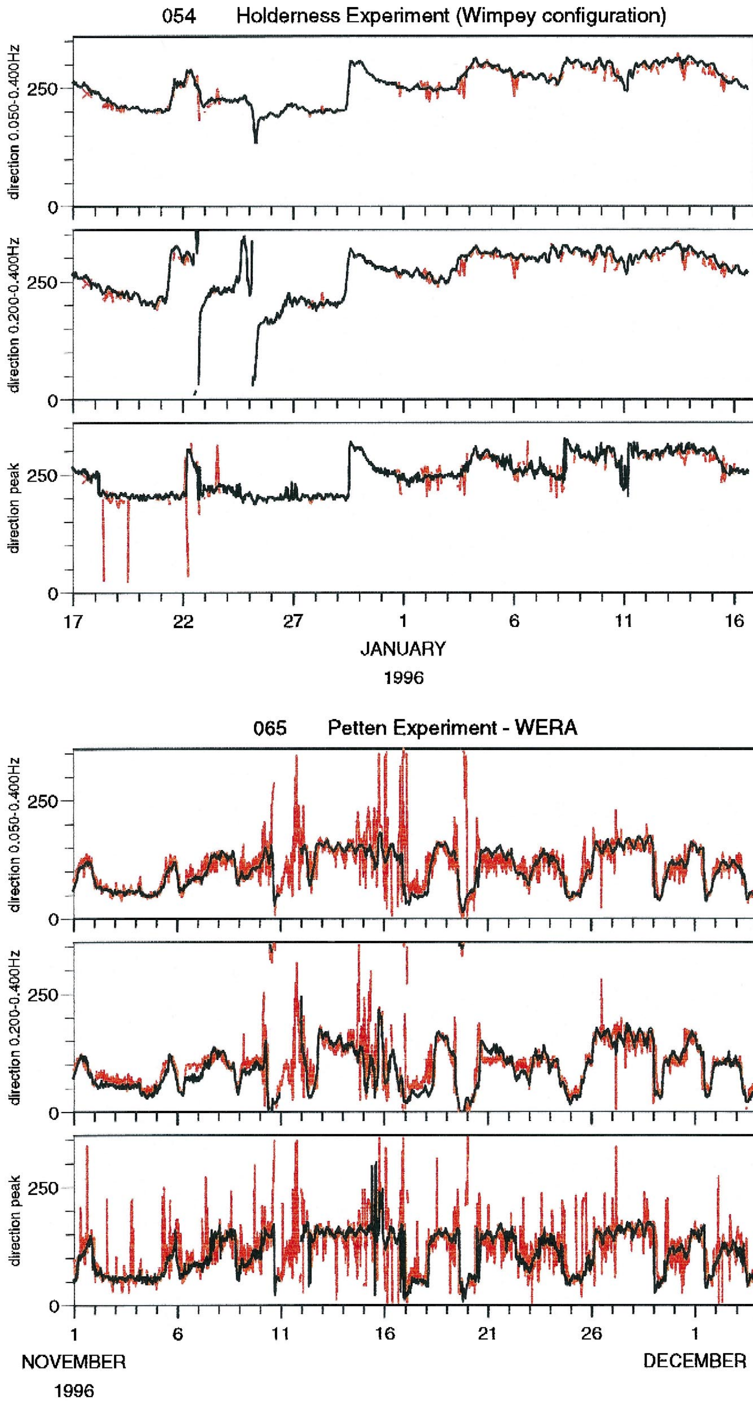


Fig. 5. As Fig. 3 for mean direction towards which the waves are propagating.

measurements are so short. Quality is judged by measuring the signal to noise of key features in the backscatter signal. Often, wave measurement is limited (both at Holderness and Petten) by current variability and/or high antenna sidelobe levels, both of which distort the first order part of the signal (Wyatt, 1994; Kingsley et al., 1997). If the distortion is particularly bad, this is detected by the signal-to-noise analysis and no inversion is carried out. Other effects of this distortion will be discussed below.

Another difference between the two experiments is the increased scatter in radar direction measurements at Petten. This is reflected in the detailed statistics discussed in Section 4 and more discussion on the origin of the difference is included there. Some of the variabilities are at times of low amplitude (also contributing to mean period variability). Variability in the peak direction, in particular, could be associated with bimodality in the spectrum with similar amplitude contributions in rather different directions and at different frequencies, thus also explaining some of the peak period variability.

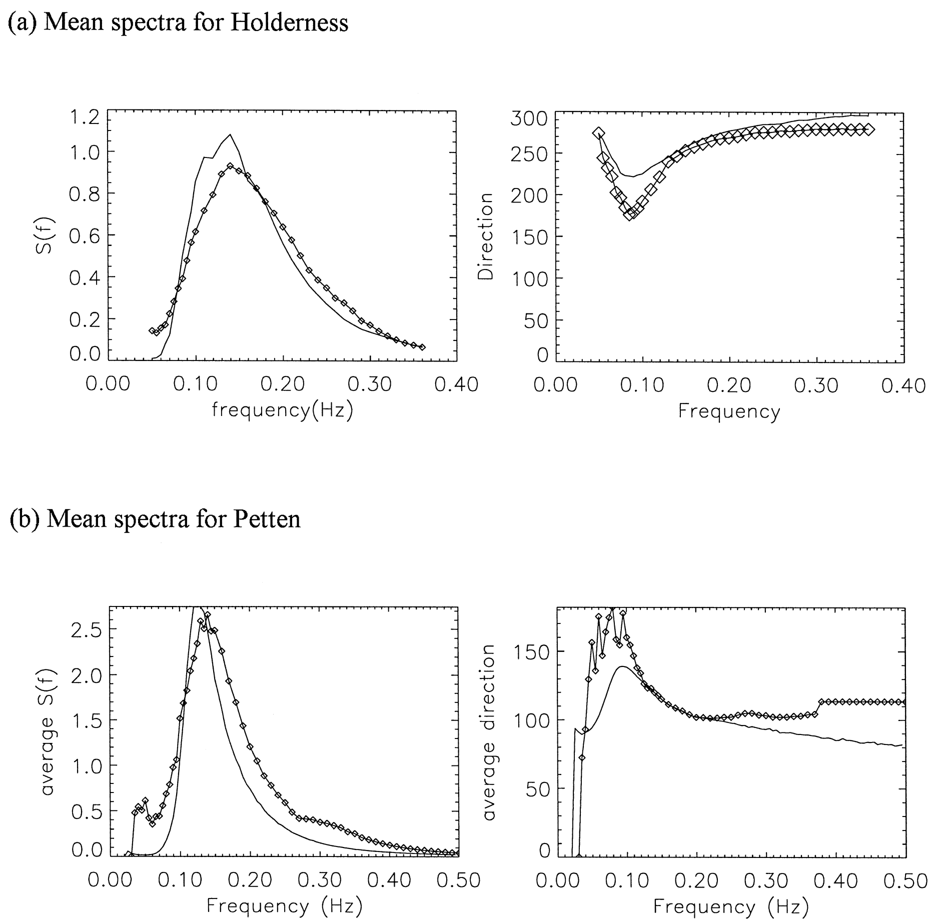


Fig. 6. Radar and buoy experiment mean frequency spectra and directions. Radar means shown with diamonds.

One feature they have in common is the overestimation in significant waveheight when it is high and this is particularly noticeable in the high frequency amplitude contributions, peak amplitude being, if anything, slightly underestimated. The overestimation of high frequency amplitude is directly related to the underestimation in mean period at these times. These features can be seen particularly clearly in Fig. 6 which shows the experiment mean frequency spectra for both instruments and experiments. The experiment mean for each instrument is the average overall measurements that are co-temporal and co-located with those of the other instrument. The figure also shows the experiment mean directions showing good agreement, especially near the peak of the radar mean spectrum, with some disagreement at lower frequencies.

## 3. Directional spectra comparisons

Comparisons of full directional spectra are discussed here. Differences provide guidance for the interpretation of the qualitative comparisons presented above and the quantitative results in Section 4. Directional frequency spectra will be used and those of the wavebuoy are estimated from the Fourier coefficients using the Lygre and Krogstad (1986) maximum entropy method. Wyatt (1997), Ewans (1998) and Krogstad et al. (1999) present evidence to support the use of maximum entropy for the interpretation of wavebuoy data and, in particular, show its use in demonstrating the existence of bimodality in the spectrum.

Fig. 7 shows eight spectra at (mostly) three hourly intervals during the development of a storm. There was just one occasion in this time sequence (at 1800 h on 1/12/96) when there was no WERA wave measurement and hence, the next 20-min measurement has been used instead. Each directional spectral pair is scaled to the maximum in the radar measurement and contours are drawn at (up to) six logarithmically spaced levels with increments from the radar peak of 0.3. Logarithmic levels have been selected to enable a clearer comparison at the high frequencies where amplitudes are relatively low. The time sequence shows the change in shape of the spectrum as the storm develops; the relative amplitudes are shown in the lower frame of the figure which also shows a comparison of significant waveheight. Wind directions are also indicated on the figures. Those on the wavebuoy plots are directions measured not at the location of the wavebuoy (and hence, not at the same place as the radar wind direction estimates) but at a site on the coast. The size of this arrow reflects the measured wind speed (the radar does not provide a reliable wind speed measurement at present).

Fig. 7. Directional spectra measured by the radar (upper panel for each group) and the directional waverider (centre panel). Contour levels are described in the text. The number next to the radar label is a measure of the convergence of the inversion procedure and values less than 2 are usually acceptable. Wind directions are shown with arrows. In the waverider plots, these are scaled according to wind speed (as measured on the coast) which is also shown next to the arrow. The lower panel shows the corresponding frequency spectra, radar is the solid line and buoy the dashed line (note the log scaling), and corresponding significant waveheights, radar above wavebuoy.

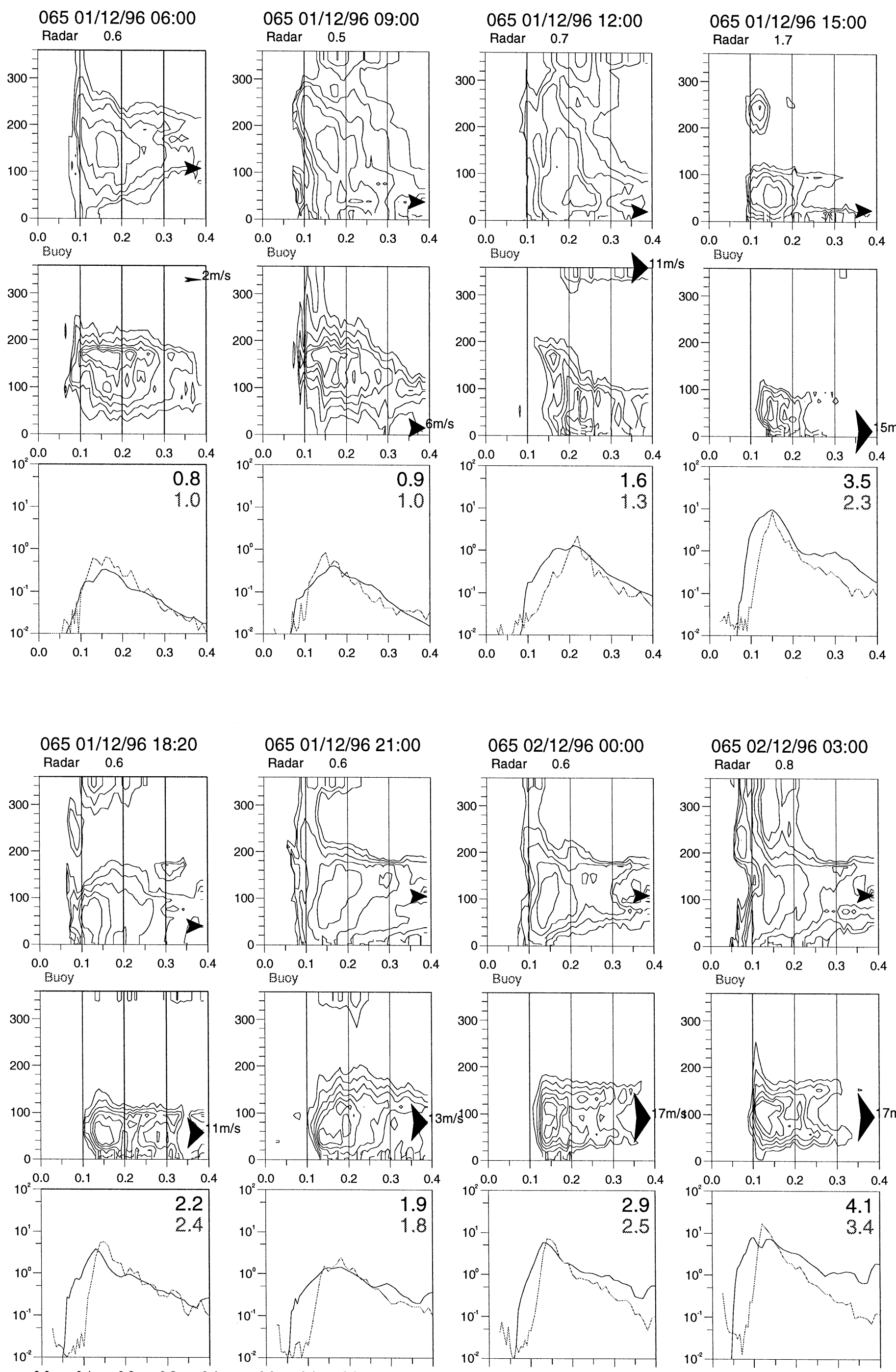
065 01/12/96 06:00
Radar 0.6
Buoy
2m/s
0.8
1.0
065 01/12/96 09:00
Radar 0.5
Buoy
6m/s
0.9
1.0
065 01/12/96 12:00
Radar 0.7
Buoy
11m/s
1.6
1.3
065 01/12/96 15:00
Radar 1.7
Buoy
15m/s
3.5
2.3
065 01/12/96 18:20
Radar 0.6
Buoy
1m/s
2.2
2.4
065 01/12/96 21:00
Radar 0.6
Buoy
3m/s
1.9
1.8
065 02/12/96 00:00
Radar 0.6
Buoy
7m/s
2.9
2.5
065 02/12/96 03:00
Radar 0.8
Buoy
7m/s
4.1
3.4

The tendency for the radar to slightly underestimate peak amplitude is clear in both the 2D and 1D plots in Fig. 7. In the 2D plots, the highest contour on most of the wavebuoy directional spectra plots marks the direction and frequency ranges of waves above the radar peak. Although this could be attributable to the known tendency of the maximum entropy method to enhance peaks, the larger peak amplitude in the wavebuoy measurements can also be seen in the frequency spectra. The radar overestimation of amplitude at high frequencies as the storm builds up is also very clear. There is also evidence of overestimation at frequencies below the peak. This latter effect is clearly related to the presence of features in the radar spectrum that are not present in the wavebuoy spectrum, e.g., the mode at $\sim 0.12$ Hz and 250° in the spectrum at 1500 h on the first of December or at $\sim 0.07$ Hz and 230° at 0300 h on the second of December. These are probably linked to the current variability and/or high sidelobe levels mentioned earlier. These produce clearly identifiable peaks in the radar backscatter spectrum which are invertible if they are more than 3 dB below the first order signal and then contribute identifiable peaks, the modes referred to above, in the resulting wave spectra.

Differences between the measurements have been identified but it is important to also stress the similarities. The shape over most of the spectrum for these and most other WERA and OSCR spectra show generally good agreement with that of the wavebuoy estimates. One feature that both spectra demonstrate particularly in the later measurements is bimodality at high frequencies. This is thought to be a feature of fetch-limited seas (Young et al., 1995; Ewans, 1998). Here, wind direction is onshore but the wave field is perhaps fetch-limited by the English coast. This aspect of the measurement merits further study. There are also occasions when the longer waves also exhibit bimodality in the wavebuoy spectrum but not (or at least not so clearly) in the radar spectrum. This is probably related to the more limited direction and frequency resolution in the radar measurements (Wyatt and Holden, 1994).

## 4. Statistical analysis

### 4.1. Methodology

The starting point for the application of the ML method is a dataset which consists of a time-ordered series of spectra measured by the radar and a directional waverider located within the region of the radar measurement. Each radar wave file (after the processing referred to in Section 1 above) contains values for the frequency spectrum, $S(f)$, mean direction, $\theta(f)$, directional spread, $\sigma(f)$, the first and second Fourier coefficients, $a_i(f)$ and $b_i(f)$ $i=1,2$, and 90% confidence intervals for $S(f)$, $\theta(f)$ and $\sigma(f)$. The confidence intervals have been determined using the results of a simulation method that determines the degrees of freedom in these radar measurements. Nine model sea-states are used to generate simulated radar spectra. All have wind sea and swell contributions with differing relative amplitudes and directions. The known sampling variability in the radar spectrum is then used to generate 5000 samples, each of which is inverted to provide an ensemble of radar wave measurements. The time taken to do this is the limiting factor in the analysis, i.e., this is the reason for the restriction to nine different models. The variances can then be estimated and analysed. The process has to be carried out in full for different radio frequencies, sampling or averaging procedure and hence, a separate analysis was required for OSCR and WERA. However, the differences found were actually quite small. The wavebuoy data files contain values for $S(f)$, $\theta(f)$ and $\sigma(f)$, and either the Fourier coefficients or values for the second harmonics of the angular power distribution from which they may be calculated. The variances of these parameters are determined using the known degrees of freedom.

Comparisons are made of parameters obtained by integrating $S(f)$ and its moments over specified frequency ranges. The variances for the integrated parameters are determined using standard techniques (Krogstad et al., 1999). Comparisons can also be made at individual frequencies but these have large variances resulting in a ML fit that has itself a large variance and hence, can only provide limited quantitative information. From the integral of $S(f)$, amplitude is calculated using the standard definition of the significant wave height, $H_S$, but restricting the frequency range of the integral ($H_S = 4[\int_{f_1}^{f_2} S(f)\mathrm{d}f]^{\frac{1}{2}}$). Mean period, for a specified frequency band, is determined from the first moment of the frequency spectrum, i.e.,

$$T_1 = \frac{\int_{f_1}^{f_2} S(f)\mathrm{d}f}{\int_{f_1}^{f_2} f S(f)\mathrm{d}f}.$$

This expression is also used to estimate peak period where the integration is carried out over a 20-mHz band around the frequency of the maximum of $S(f)$. The sampling variability of the radar-measured peak period has not been determined and so the ML analysis is not carried out for this parameter. The sampling variability based on the use of the $T_1$ formulation is not appropriate. Mean direction, for a specified frequency band, is determined using:

$$\theta_m = \tan^{-1} \frac{\int_{f_1}^{f_2} S(f) \sin\theta(f)\mathrm{d}f}{\int_{f_1}^{f_2} S(f) \cos\theta(f)\mathrm{d}f}.$$

Note that these expressions also define the parameters over the full range of measured frequencies which provides the conventional measure of significant wave height and mean period. Krogstad et al. (1999) discuss the ML analysis for these full range parameters. The figures are also included here for completeness.

A scatter plot of the paired data is fitted with a ML estimate of the best straight line fit through the data, assuming a normal distribution for the data. An iterative technique is needed to estimate the slope, $b$, and intercept, $a$, for the amplitude and mean period relationships. Having obtained the slope and intercept for $H_S$ and mean period, the bias of the radar relative to the wavebuoy for each parameter is computed. This is given by:

$$y_{\mathrm{rel}} = \frac{a + (b-1)x}{x},$$

where $x$ spans the range of the wavebuoy data. The 95% confidence intervals for the relative bias are given by:

$$y_{\mathrm{rel}} \pm 1.96\sqrt{\frac{\mathrm{var}(a)}{x^2} + \mathrm{var}(b) + \frac{2\mathrm{cov}(a,b)}{x}}\ .$$

These are used to assess the statistical significance of any bias that might be suggested by, e.g., $b > 1$. If zero bias for a particular parameter falls within the confidence interval for the relative bias for a specified range of frequencies, then we can assert that the experiment provides no evidence of bias for that parameter over that range.

When comparing mean directions, it is sufficient to apply the method to the directional difference and assume that this has a normal distribution. The ML estimate of the mean difference is obtained by using the summed, integrated variances for the radar and wavebuoy, $\sigma_j^2$, to weight the individual direction differences, $\psi_j$, which are then included in a weighted mean, $\hat{\mu}$.

$$\hat{\mu} = \frac{\sum_{j=1}^{n} \frac{\psi_j}{\sigma_j^2}}{\sum_{j=1}^{n} \frac{1}{\sigma_j^2}}\ .$$

The variance of $\hat{\mu}$ is given by:

$$\mathrm{var}(\hat{\mu}) = \frac{1}{\sum_{j=1}^{n} \frac{1}{\sigma_j^2}}\ ,$$

and hence, 95% confidence intervals for the mean difference can be determined.

The results of this analysis will be compared with more standard statistical parameters, i.e., relative bias and variance when considering amplitude and mean period, and bias and variance for direction using direction differences. These are the standard statistics identified as being most useful for wave measurement comparisons in (Krogstad et al., 1999). However, in that paper, they were shown to provide a less useful measure of bias than is obtained with the ML analysis.

### *4.2. Results*

We present comparisons of the radar and wavebuoy data integrated over the whole experimental range 0.05–0.4 Hz, over a 20-mHz frequency range centred on the maximum amplitude in each individual spectra (hereafter referred to as 'peak'), and over the following frequency bands: 0.05–0.1 Hz, 0.1–0.15 Hz, 0.15–0.2 Hz, 0.2–0.3 Hz, 0.3–0.4 Hz.

#### *4.2.1. Qualitative analysis*

Fig. 8 shows the scatter plots with 90% confidence intervals for the full range and peak bands for the Holderness and Petten experiments. The ML fits are shown except

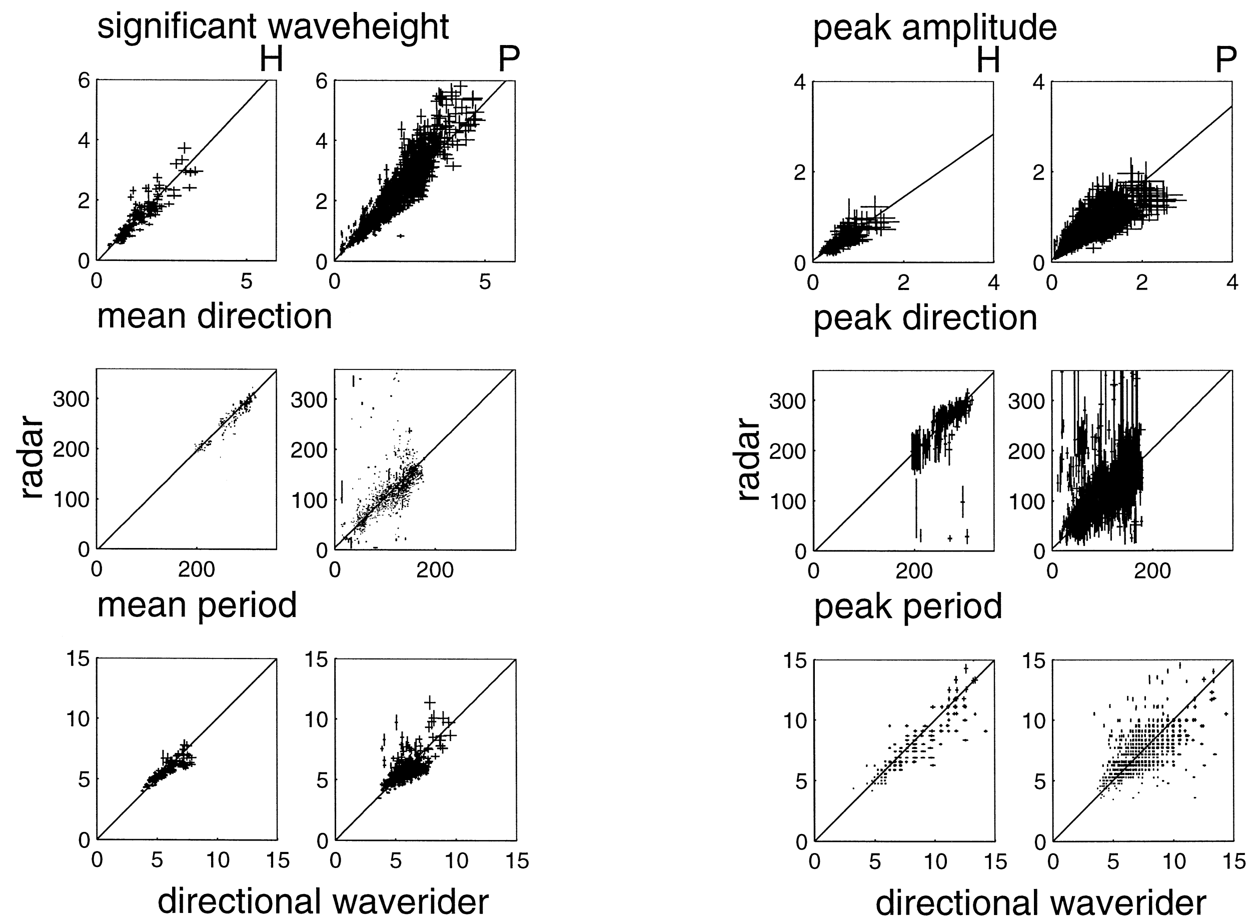


Fig. 8. Wave parameters measured at Holderness (H) and Petten (P). 90% confidence intervals are shown. The ML lines are shown in all cases except for the peak period comparisons.

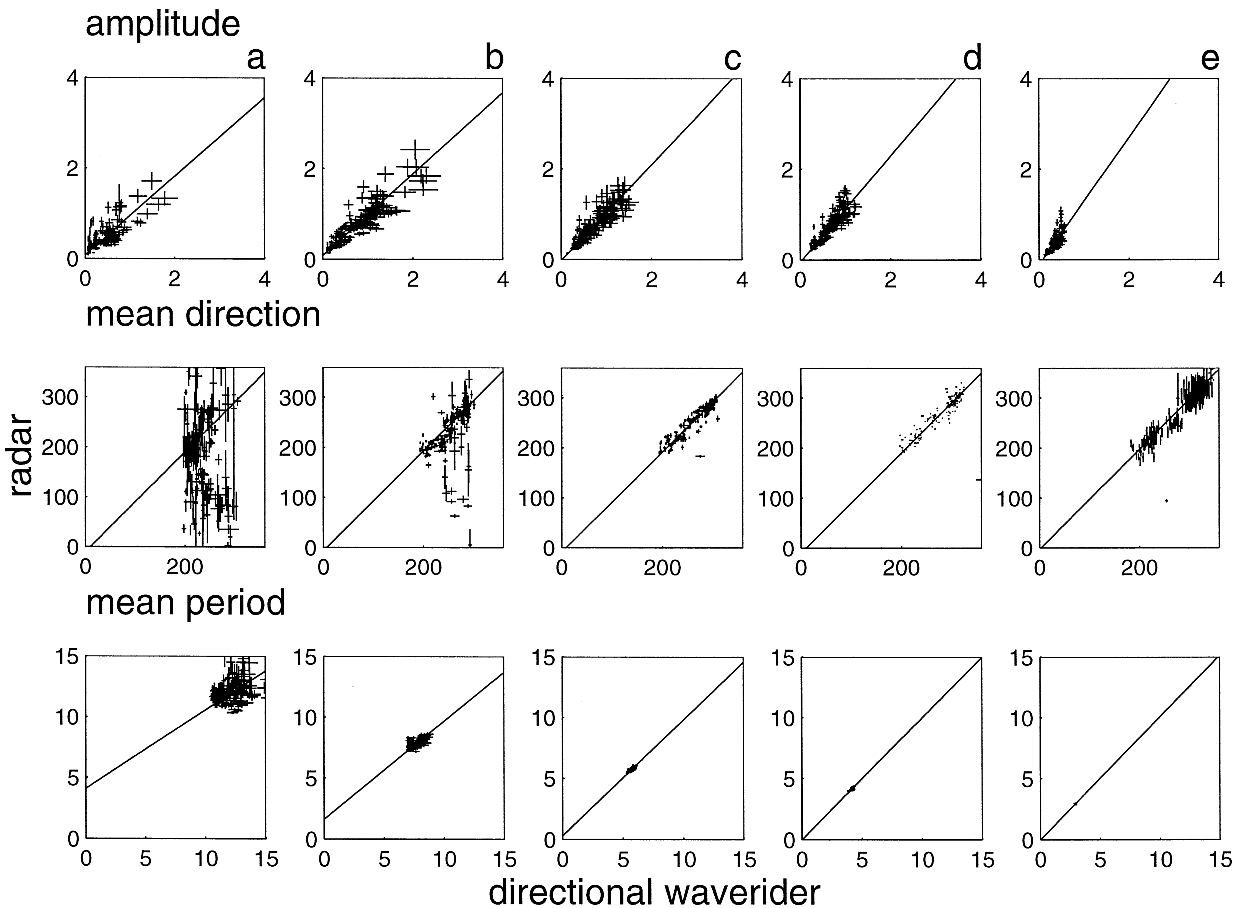


Fig. 9. Wave parameters measured at Holderness. Frequency bands: (a) 0.05–0.1 Hz, (b) 0.1–0.15 Hz, (c) 0.15–0.2 Hz, (d) 0.2–0.3 Hz, (e) 0.3–0.4 Hz.

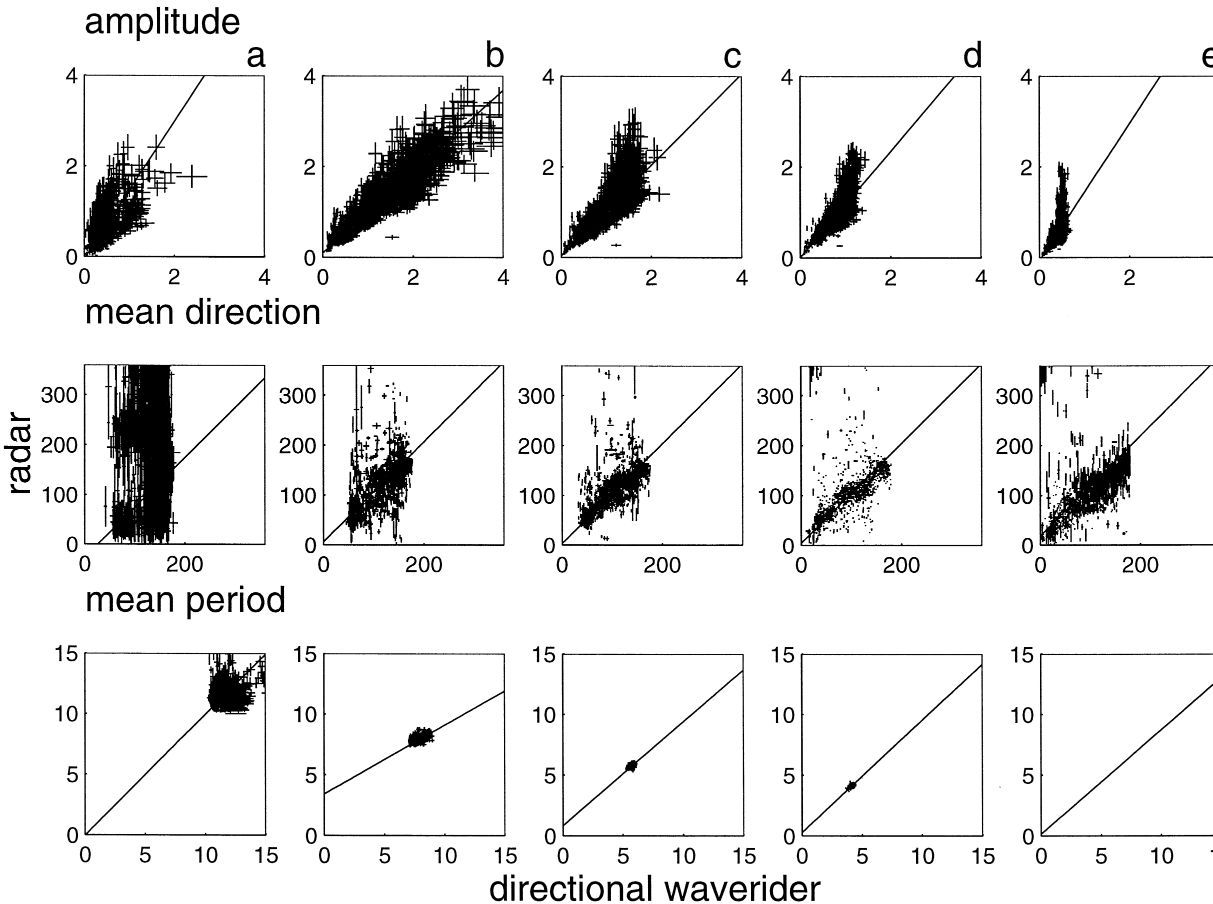


Fig. 10. Wave parameters measured at Petten, otherwise as Fig. 9.

Table 1
Holderness2 amplitude comparison. ML biases are coded as: (+4) >15%, (+3) 10–15%, (+2) 5–10%, (+1) 0–5%, (0) 0% and similar for negatives

| Frequency (Hz) | Relative error (%) | Standard deviation (%) | Slope ($b$) | Intercept ($a$) | ML bias amplitude low | ML bias amplitude high | Zero bias range (m) |
|---|---|---|---|---|---|---|---|
| 0.05–0.1 | 92 | 121 | 0.872 | 0.078 | +3 | −1 | 0.5–0.7 |
| 0.1–0.15 | 23 | 53 | 0.900 | 0.082 | +3 | −1 | 0.7–1.0 |
| 0.15–0.2 | 1 | 23 | 1.060 | −0.027 | −1 | +1 | 0.4–0.65 |
| 0.2–0.3 | 4 | 23 | 1.171 | −0.053 | −1 | +2 | 0.25–0.35 |
| 0.3–0.4 | 6 | 39 | 1.407 | −0.114 | −3 | +3 | 0.27–0.29 |
| Peak | −9 | 22 | 0.700 | 0.039 | −3 | −4 | n/a |
| **0.05–0.4** | **1** | **18** | **1.062** | **−0.064** | **−1** | **+1** | **0.9–1.3** |

for the case of peak period where the analysis was not performed and the line of slope unity was drawn instead. The significant waveheight comparisons show good correlation with some indication of overestimation by the radar in high sea-states when confidence intervals are also wider. The underestimation in peak amplitude, commented on earlier, is clearly seen in both experiments. Mean and peak directions at Holderness are in very good agreement. There is rather more scatter in the Petten dataset particularly for peak direction where it can be seen that the confidence intervals are rather wide for the cases with largest differences. The different ranges in direction are related to the geographical location of the two sites. Mean and peak period are also well-correlated. Some of the scatter in the Petten case can be attributed to the same cause as the scatter in peak direction, i.e., to the presence of spurious peaks in the spectrum (mostly at low frequencies) due to antenna sidelobes and/or current variability.

The scatter plots, confidence intervals and fits for the other frequency bands are shown in Fig. 9 for Holderness and Fig. 10 for Petten. The overestimation of short-wave amplitude is seen very clearly in the Petten dataset (Fig. 10c–e). The scatter in low frequency direction is very clear for both experiments and is present to a lesser degree across all frequencies in the Petten dataset. The scatter at higher frequencies is likely to

Table 2
Petten amplitude comparisons

| Frequency (Hz) | Relative error (%) | Standard deviation (%) | Slope ($b$) | Intercept ($a$) | ML bias amplitude low | ML bias amplitude high | Zero bias range (m) |
|---|---|---|---|---|---|---|---|
| 0.05–0.1 | 107 | 135 | 1.517 | −0.048 | +4 | +4 | n/a |
| 0.1–0.15 | 16 | 43 | 0.896 | 0.093 | +1 | −2 | 0.85–1.0 |
| 0.15–0.2 | 11 | 31 | 1.002 | 0.036 | +2 | +1 | n/a |
| 0.2–0.3 | 20 | 30 | 1.171 | 0.001 | +4 | +4 | n/a |
| 0.3–0.4 | 49 | 53 | 1.511 | −0.066 | +4 | +4 | n/a |
| Peak | 1 | 51 | 0.852 | 0.046 | +1 | −3 | 0.28–0.35 |
| **0.05–0.4** | **15** | **28** | **1.050** | **0.017** | **+3** | **+1** | **n/a** |

Table 3
Holderness2 mean period comparisons. ML biases are coded as: (+4) >15%, (+3) >10%, (+2) 5–10%, (+1) 0–5%, (0) 0% and similar for negatives

| Frequency (Hz) | Relative error (%) | Standard deviation (%) | Slope ($b$) | Intercept ($a$) | ML bias $T$ low | ML bias $T$ high |
|---|---|---|---|---|---|---|
| 0.05–0.1 | 3 | 8 | 0.647 | 4.083 | +1 | −2 |
| 0.1–0.15 | 2 | 4 | 0.806 | 1.614 | +1 | −1 |
| 0.15–0.2 | 0 | 2 | 0.953 | 0.276 | +1 | 0 |
| 0.2–0.3 | 0 | 2 | 1.001 | −0.021 | 0 | 0 |
| 0.3–0.4 | −1 | 3 | 1.012 | −0.021 | 0 | 0 |
| **0.05–0.4** | **1** | **8** | **0.765** | **1.252** | **+2** | **−2** |

be due to inadequacies in the scatter model in high sea-states. Additional high frequency modes are often seen in the directional spectra in these conditions. The increased confidence intervals seen in the highest frequency band (e) reflect the fact that the inversion only partly covers the band, the rest being described by a high frequency tail.

#### 4.2.2. Quantitative analysis

Tables 1–6 summarize the results of the statistical analysis for all bands and the three parameters: amplitude, period and direction. Note that positive biases indicate that the radar overestimates the parameter relative to the wavebuoy. Positive direction differences indicate that the radar direction estimate is larger in the clockwise sense.

*4.2.2.1. Amplitude*. The ML bias figures included in the tables were obtained using figures, such as Fig. 11, that show the relative bias and confidence intervals for significant waveheight (bold in the tables) for the two experiments. The figure shows that there is no evidence for a bias in significant wave height greater than ±5% for values above 0.5 m in the Holderness experiment. In this case, the range of $H_S$ for which there is no evidence of bias, i.e., that range where zero relative bias lies between the upper and lower confidence intervals, is 0.9–1.3 m. However, the bias is larger and positive in the Petten experiment in the lower sea-state conditions. It seems likely that this is due to low frequency amplitude overestimation which is significantly biased in this experiment due to a greater impact of short time scale current variability and/or

Table 4
Petten period comparisons

| Frequency (Hz) | Relative error (%) | Standard deviation (%) | Slope ($b$) | Intercept ($a$) | ML bias $T$ low | ML bias $T$ high |
|---|---|---|---|---|---|---|
| 0.05–0.1 | 5 | 8 | 0.996 | −0.024 | 0 | 0 |
| 0.1–0.15 | 1 | 4 | 0.566 | 3.414 | 0 | −1 |
| 0.15–0.2 | 0 | 2 | 0.857 | 0.818 | +1 | −1 |
| 0.2–0.3 | −1 | 2 | 0.926 | 0.279 | 0 | −1 |
| 0.3–0.4 | −1 | 2 | 0.958 | 0.139 | 0 | 0 |
| **0.05–0.4** | **0** | **13** | **0.597** | **2.043** | **+2** | **−4** |

Table 5
Holderness2 mean direction comparisons in degrees

| Frequency (Hz) | Mean $\Delta\theta$ | Standard deviation | ML $\Delta\theta$ |
|---|---|---|---|
| 0.05–0.1 | −7.3 | 58.3 | −9.9 |
| 0.1–0.15 | −8.9 | 26.0 | −6.9 |
| 0.15–0.2 | −5.9 | 8.0 | −8.7 |
| 0.2–0.3 | −6.7 | 9.4 | −10.5 |
| 0.3–0.4 | −10.5 | 13.2 | −2.5 |
| Peak | −2.1 | 22.1 | −3.3 |
| **0.05–0.4** | **−6.6** | **7.7** | **−3.5** |

antenna sidelobes. In high sea-states, the bias at Petten is down to +5%, roughly the same figure as at Holderness.

The relative error of +1% for peak amplitude at Petten is not consistent with the comments made earlier about underestimation of the peak on average. This underestimation is revealed in the high amplitude ML bias of −10–15%. The overestimation in relative error is probably due to the same factors that led to an overestimation in the ML bias in low sea-states and again is attributable to current variability and/or antenna sidelobes at Petten. At Holderness, the relative error (−9%) seems to underestimate the larger negative bias found with the ML method (> 15% at the higher sea-states). This is probably due to the same factors since the lower frequencies in the radar measurements are most affected and these have larger variances and therefore carry less weight in the ML analysis.

Note that the standard relative error estimates have not been subdivided into amplitude ranges. This would be possible of course, but with the ML approach, this information emerges automatically. The variation in standard deviation from band to band is partially reflecting the amplitude-related variations in bias in each band.

The overestimation of amplitude at high frequencies at Petten (seen in Figs. 3 and 6) is ~17% for 0.2–0.3 Hz and higher at higher frequencies. This is directly attributable to limitations in the scattering theory in high sea-states (Wyatt, 1995) when the small slope assumption becomes invalid and the backscattered power is much higher than is predicted by the theory.

Table 6
Petten mean direction comparisons in degrees

| Frequency (Hz) | Mean $\Delta\theta$ | Standard deviation | ML $\Delta\theta$ |
|---|---|---|---|
| 0.05–0.1 | −5.3 | 57.9 | −25.9 |
| 0.1–0.15 | 1.8 | 22.0 | 6.4 |
| 0.15–0.2 | 2.4 | 19.2 | 3.3 |
| 0.2–0.3 | 3.3 | 20.0 | 4.1 |
| 0.3–0.4 | 4.1 | 21.8 | 19.1 |
| Peak | 2.6 | 29.7 | 4.0 |
| **0.05–0.4** | **0.6** | **18.6** | **3.8** |

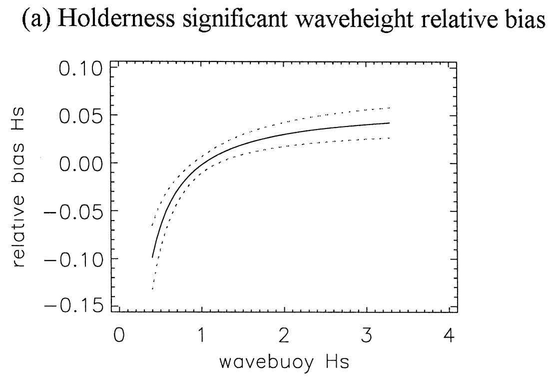


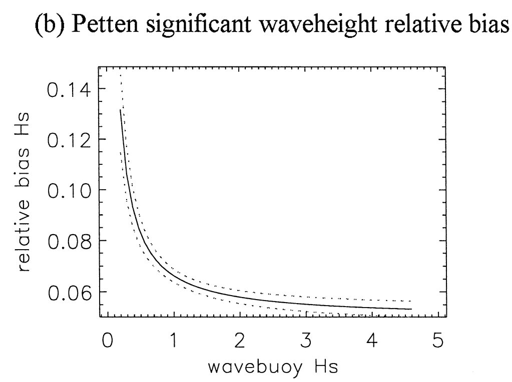


Fig. 11. Fractional significant waveheight relative bias for the two experiments shown with a solid line. The 95% confidence limits are shown with dotted lines.

It is noticeable that although the relative errors are different from experiment to experiment, the ML slopes are rather similar over most of the frequency ranges. It is possible therefore that the ML analysis could provide a robust mechanism for calibrating the data to improve the performance of the system pending improvements in the inversion algorithms or scattering model.

As has already been noted, the largest amplitude biases are at high frequencies. An alternative approach to a calibration based on these biases would be to reduce the frequency range, for which a full inversion is carried out, in proportion to significant waveheight. The model used for high frequencies would thus be extended to lower frequencies.

*4.2.2.2. Period.* The period comparisons presented in Tables 3 and 4 are less easy to interpret and for many bands, are not especially useful because, of course, the range of periods can be rather small. Biases are anyway generally rather small. Of most interest is the comparison of mean period over the full frequency range (shown in bold on the tables). Once again, the standard relative error calculation does not reveal the variation in bias with wavebuoy period. The larger variation in this for the Petten data over the full range is reflected in the standard deviation. When the wavebuoy period is low, the positive bias is related to the overestimation in low frequency amplitude which had an impact on significant waveheight in low sea-states and was discussed above. The underestimation in period when the wavebuoy measures a high mean period is associated with the overestimation in amplitude at high frequencies in high sea-states. As can be seen, this effect is more noticeable at Petten where the number of such events was larger. Although the ML parameter estimates are not the same for period from experiment to experiment, since there is obviously a direct link between the period and amplitude biases, one would not want to calibrate for period independently. A calibration on the basis of the amplitude ML analysis should deal with the period problems identified here.

*4.2.2.3. Direction.* Biases in mean direction (Tables 5 and 6) are within 15° for the Holderness experiment with rather larger differences at the frequency extremes for the Petten experiment. Confidence intervals for the ML estimates are all less than 1°. The large standard deviations at low frequencies for both experiments reflect the bimodality in the radar measurements due to spurious spectral contributions from surface current variability and/or antenna sidelobes. The ML biases present a similar picture to the standard mean differences presented in the tables. As was seen in Fig. 10, there is rather more scatter in the directions measured at Petten at higher frequencies which is reflected in the increased standard deviations beyond 0.15 Hz. Averaged over the whole frequency range (in bold), the ML bias is negative at Holderness and positive but roughly the same magnitude at Petten, perhaps reflecting the different geographical locations, Holderness being on the west and Petten on the east of the Southern North Sea.

*4.2.3. Summary*

The results of this analysis can be summarised as follows.

(1) The radar measurements underestimate the amplitude of the spectral peak. Since this is not linked to a corresponding underestimation in significant waveheight, a possible reason is a poorer frequency resolution in the radar measurements associated with the inversion procedure (which includes a certain amount of averaging).

(2) The radar measurements overestimate high frequency amplitude in high sea-states. This leads to an overestimation in $H_S$.

(3) The radar measurements overestimate amplitude below the peak due to spurious contributions to the spectrum caused by antenna sidelobes and current variability.

(4) The ML analysis provides bias estimates that are more consistent from experiment to experiment and with qualitative comparisons of directional spectra than those obtained using simpler statistical techniques, e.g., relative error.

(5) Differences between radar and wavebuoy measurements of period can be related to differences in the distribution of energy with frequency, i.e., to the differences in peak and high frequency amplitudes.

(6) At low frequencies, radar-measured mean directions are not very reliable.

(7) At high frequencies, radar-measured mean directions appear to be less reliable in higher sea-states.

## 5. Discussion and conclusions

In this paper, we have presented qualitative and quantitative evidence of the advantages and limitations of HF radar for monitoring ocean waves in coastal waters. Directional spectra are obtainable every hour with OSCR and 20 min with WERA at ranges up to 20 km from the coast providing detailed measurements of the spatial variability of the coastal wave field. During the Petten experiment, measurements were available more or less continuously over a period of more than a month. The limitations that have been identified, by comparisons of particular parameters or of the full directional spectrum, are associated with short time or space scale current variability and/or antenna sidelobes. Both of these are the subject of research at Sheffield. One other limitation is the problem of applying the inversion based on a theory that is clearly invalid in high sea-states at the operating frequencies of OSCR and WERA. This has been shown to lead to a substantial overestimation in amplitude at high frequencies. One suggestion for dealing with this is the calibration approach using ML relationships. An alternative is to limit the frequency range of the inversion and parameterise the amplitude at high frequencies with, e.g., a $f^5$ spectral tail. Of course, the most satisfactory solution would be to develop a theory that explains the observed backscatter in high seas conditions. This is the subject of investigation at Sheffield.

We have demonstrated that it is possible and important to include the variability associated with both radar and wavebuoy in an analysis of their relative performance as wave measuring systems. This has allowed detailed quantitative intercomparisons to be made. The analysis reported here for the OSCR system has revealed that in certain frequency bands and for certain amplitude ranges, there exists no bias between the two measurement systems. However, the maximum significant waveheight at Holderness was only 3.5 m. At Petten, there were periods of higher waveheights and the amplitude biases tended to be larger. However, although the amplitude bias estimates for the two very different experiments using very different radar systems are different, the ML relationships between radar and wavebuoy amplitude found are similar. The provision of this type of data opens up the possibility of producing calibration/correction curves for radar measurements that could be used until more accurate parameter extraction methods are developed.

Direction biases over most of the frequency range of less than 15° and are within the nominal directional resolution in the Sheffield inversion process. Except at the extremes, the relative biases in amplitude estimation are within $\pm 10\%$ for the frequency bands analysed here and $\pm 5\%$ for significant waveheight. These ranges are certainly adequate for many operational purposes.

## Acknowledgements

This work was partly funded by the EC MAST programme (MAS2CT940103) and by MAFF under the Flood Protection Commission FD0306 with the Proudman Oceanographic Laboratory and NERC contract F3CR07-G1-02. We are particularly grateful to Louise Ledgard who collected and processed the OSCR data and to the SCAWVEX team at the University of Hamburg who collected the WERA data.

## References


Ewans, K.C., 1998. Observations of the directional spectrum of fetch-limited wave. J. Phys. Oceanogr. 28, 495–512.

Gurgel, K.-W., Antonischki, G., 1997. Remote sensing of surface currents and waves by the HF radar WERA. Proceedings of the 7th International Conference on Electronic Engineering in Oceanography, Southampton, Vol. 439. IEE Conference Publication, June 1997, pp. 211–217.

Gurgel, K.-W., Antonischki, G., Essen, H.-H., Schlick, T., 1999. Wellen Radar (WERA), a new ground-wave based HF radar for ocean remote sensing. Coastal Eng., this issue.

Hisaki, Y., 1996. Nonlinear inversion of the integral equation to estimate ocean wave spectra from HF radar. Radio Science 31, 25–39.

Holden, G.J., Wyatt, L.R., 1992. The extraction of sea-state in shallow water using HF radar. IEE Proceedings 139, 175–181, Part F.

Isaac, F.E., Wyatt, L.R., 1997. Segmentation of HF radar measured directional wave spectra using the Voronoi Diagram. Journal of Atmospheric and Oceanic Technology 14, 950–959.

Kingsley, S.P., Blake, T.M., Fisher, A.J., Ledgard, L.J., Wyatt, L.R., 1997. Dual HF radar measurements of sea waves from straight coastlines. Proceedings of 7th International Conference on HF Radio Systems and Techniques, Nottingham. IEE, London, UK, July 1997.

Krogstad, H.E., Wolf, J., Thompson, S.P., Wyatt, L.R., 1999. Methods for the intercomparison of wave measurements. Coastal Eng., this issue.

Lygre, A., Krogstad, H.E., 1986. Maximum entropy estimation of the directional distribution in ocean wave spectra. J. Phys. Oceanogr. 16, 2052–2060.

Paduan, J.D., Graber, H.C., 1997. Introduction to high frequency radar: reality and myth. Oceanography 10 (2), 36–39.

Prandle, D., Baillard, G., Banaszek, A., Bell, P., Flatt, D., Hardcastle, P., Harrison, A., Humphrey, J., Holdaway, G., Lane, A., Player, R., Williams, J., Wolf, J., 1996. The Holderness Coastal Experiment '93–'96, POL Report 44. Proudman Oceanographic Laboratory, UK.

Sova, M.G., 1995. The sampling variability and the validation of high frequency wave measurements of the sea surface. PhD thesis (unpublished), University of Sheffield.

Wyatt, L.R., 1990a. Progress in the interpretation of HF sea echo: HF radar as a remote sensing tool. IEE Proceedings 137, 139–147.

Wyatt, L.R., 1990b. A relaxation method for integral inversion applied to HF radar measurement of the ocean wave directional spectrum. International Journal of Remote Sensing 11, 1481–1494.

Wyatt, L.R., 1994. Coastal surface current and wave measurement with HF radar: limitations and prospects. In: Beven, K., Chatwin, P.C., Millbank, J.H. (Eds.), Mixing and Transport in the Environment. Wiley, New York, pp. 295–306.

Wyatt, L.R., 1995. High order nonlinearities in HF radar backscatter from the ocean surface. IEE Proceedings: Radar, Sonar and Navigation 142, 293–300.

Wyatt, L.R., 1996. Non-linear inversion of HF radar backscatter. SCEOS technical note, EPSRC/JA/1, University of Sheffield.

Wyatt, L.R., 1997., Holderness2 OSCR and wavebuoy directional spectra comparisons, SCAWVEX technical note, SCAW-tec17, University of Sheffield.

Wyatt, L.R., Holden, G.J., 1992. Developments in ocean wave measurement by HF radar. IEE Proceedings 139 (2), 170–174.

Wyatt, L.R., Holden, G.J., 1994. Limits in direction and frequency resolution for HF radar ocean wave directional spectra and measurement. The Global Atmosphere and Ocean System 2, 265–290.

Wyatt, L.R., Ledgard, L.J., 1996. OSCR wave measurements: some preliminary results. IEEE J. Oceanic Eng. 21, 64–76.

Wyatt, L.R., Ledgard, L.J., Anderson, C.W., 1997. Maximum likelihood estimation of the directional distribution of 0.53 Hz ocean waves. Journal of Atmospheric and Oceanic Technology 14, 591–603.

Young, I.R., Verhagen, L.A., Banner, M.L., 1995. A note on the bimodal directional spreading of fetch-limited waves1. J. Geophys. Res. 100, 773–778.